

A comparison of exact quantum mechanical and various semiclassical treatments for the vibronic absorption spectrum: The case of fast vibrational relaxation

Eran Rabani, S. A. Egorov,^{a)} and B. J. Berne

Department of Chemistry, Columbia University, 3000 Broadway, New York, New York 10027

(Received 9 June 1998; accepted 17 July 1998)

We have extended our study of the vibronic absorption spectrum in condensed matter [S. A. Egorov, E. Rabani, and B. J. Berne, *J. Chem. Phys.* **108**, 1407 (1998)] to the case when the electronic dephasing rate is slow compared to the vibrational relaxation rate in both electronic states. We find that under such circumstances, unlike the case of fast electronic dephasing, treating all nuclear degrees of freedom classically provides better agreement with the exact quantum treatment than the mixed quantum-classical approximation. These results are consistent with the conclusions reached by Bader and Berne in their study of mixed quantum-classical treatments of vibrational relaxation processes. © 1998 American Institute of Physics. [S0021-9606(98)51439-0]

I. INTRODUCTION

The electronic spectroscopy of chromophores embedded in crystalline or liquid hosts is a valuable tool for studying structure and dynamics of condensed matter environments. The effect of the solvent on the chromophore is reflected in the shifts and the broadening of individual spectral lines comprising the gas phase spectrum of the solute. As such, the electronic absorption spectra in condensed phases have received much attention.¹⁻³

Accurate quantum mechanical calculations of such spectra are extremely difficult to perform in view of the large number of degrees of freedom involved. Hence, various approximate treatments have been proposed in the literature over the years.⁴⁻¹⁶ In our previous study,¹⁷ we have assessed the accuracy of semiclassical treatments by studying an exactly solvable model for which both quantum mechanical and semiclassical results can be obtained exactly. This model consists of a harmonic diatomic molecule bilinearly coupled to a harmonic bath with different coupling strengths in the two electronic states of the molecule. Having performed various semiclassical calculations for this model, we have found that the best overall agreement with the exact quantum results was obtained when the vibrational coordinate of the diatomic (together with its two electronic states) was treated quantum mechanically, while the nuclear dynamics of the bath was treated classically. At first glance, this result seems to contradict the conclusions reached by Bader and Berne,¹⁸ and by others,^{19,20} in the study of vibrational energy relaxation in a similar system, where it was found that the fully classical treatment of nuclear dynamics was superior to the mixed approach described above. The origin of this controversy lies in the fact that the range of parameters studied in our previous work¹⁷ corresponds to the electronic dephasing rate being much faster than the vibrational energy relaxation

rate in either of the two electronic states. Hence, the vibrational relaxation processes did not have much influence on the vibronic absorption spectrum.

The purpose of the present work is to extend our previous study by considering the range of parameters where the vibrational relaxation rate is larger than the electronic dephasing rate. In this case, one would expect the mixed quantum-classical treatment to become inferior to the fully classical treatment of nuclear dynamics, as indeed will be shown below. The paper is organized as follows: in Sec. II we briefly describe our model, in Sec. III we review various approaches to calculating the electronic absorption spectrum, and in Sec. IV we present our results. Section V concludes.

II. MODEL

The model described herein is identical to the one used in our previous study of the vibronic absorption spectrum.¹⁷ We consider the problem of calculating the absorption spectrum of a diatomic molecule with a fixed orientation (referred to hereafter as the system), coupled to a bath. We focus on a pair of electronic states which give rise to the electronic transition when the system goes from the ground electronic state (denoted by $|0\rangle$) to the excited electronic state (denoted by $|1\rangle$). The system vibrational mode is treated in the harmonic approximation, and the bath is modeled by a collection of harmonic oscillators. The coupling between the system and the bath is taken to be linear both in the system and in the bath vibrational coordinates. However, in order to describe the electronic dephasing processes properly, the coupling coefficients are taken to be different for the two electronic states.

In the Born–Oppenheimer approximation, the total Hamiltonian can be written as

$$H = H_0|0\rangle\langle 0| + H_1|1\rangle\langle 1|, \quad (1)$$

where H_0 (H_1) is the Hamiltonian for the nuclear degrees of freedom of the system and the bath, corresponding to the

^{a)}Present address: Theoretical Chemistry Institute and Department of Chemistry, University of Wisconsin, Madison, Wisconsin 53706.

motion on the Born–Oppenheimer potential surface when the system is in its ground (excited) electronic state.

The ground and excited state Hamiltonians read,

$$H_0 = h_0(q) + H_b(\mathbf{Q}) + V_0(q, \mathbf{Q}), \quad (2)$$

and

$$H_1 = h_1(q) + H_b(\mathbf{Q}) + V_1(q, \mathbf{Q}) + \hbar \omega_e. \quad (3)$$

In Eq. (3), $\hbar \omega_e$ is the gas phase electronic transition energy of the diatomic molecule (for convenience we set it equal to 0). $h_0(q)$ and $h_1(q)$ are the system Hamiltonians for the ground ($|0\rangle$) or excited ($|1\rangle$) electronic states, respectively,

$$h_{0,1}(q) = \frac{1}{2} p^2 + \frac{1}{2} \omega_{0,1}^2 (q - q_{0,1})^2, \quad (4)$$

where q is the system mass-weighted coordinate with the frequency ω_0 and equilibrium position q_0 for state $|0\rangle$ and frequency ω_1 and equilibrium position q_1 for state $|1\rangle$; p is the conjugate momentum of q .

The bath Hamiltonian in the harmonic approximation takes the form

$$H_b(\mathbf{Q}) = \frac{1}{2} \sum_{\alpha}^{N_b} P_{\alpha}^2 + \frac{1}{2} \sum_{\alpha}^{N_b} \omega_{\alpha}^2 Q_{\alpha}^2, \quad (5)$$

where the summation index α labels the bath mass-weighted coordinates Q_{α} with conjugate momenta P_{α} , and frequencies ω_{α} ; N_b is the number of bath modes.

As mentioned earlier, the system–bath coupling is taken to be linear both in the system and in the bath coordinates

$$V_{0,1}(q, \mathbf{Q}) = \sum_{\alpha}^{N_b} g_{\alpha}^{0,1}(q - q_{0,1}) Q_{\alpha}, \quad (6)$$

where g_{α}^0 (g_{α}^1) are the coupling strengths for the ground (excited) electronic states, which we assume to be different for the two electronic states.

The reduced dynamics of the system in our model is completely determined by the two spectral densities, for the ground and excited electronic states. We restrict ourselves to the treatment of monatomic hosts, in which case we need to consider only acoustic phonons; the conventional choice of spectral density for acoustic phonons is the Debye model coupled with the deformation potential approximation,¹⁷ which gives a spectral density that is proportional to ω^3 , and has a sharp cutoff at the Debye frequency. For numerical convenience the model can be slightly modified¹⁷ by introducing a smooth exponential cutoff

$$J_{0,1}(\omega) = \rho_{0,1} \frac{\gamma^4}{6} \omega^3 \exp(-\gamma \omega). \quad (7)$$

For simplicity we use the same functional form for the two spectral densities; however, they differ by an overall system–bath coupling strength ($\rho_{0,1}$). We follow the procedure outlined in our previous work to obtain the coupling coefficients that mimic the appropriate continuous spectral density.¹⁷ This leads to the following relation between the coupling coefficients $g_{\alpha}^{0,1}$ and the spectral density $J_{0,1}$:

$$(g_{\alpha}^{0,1})^2 = 2 \omega_{\alpha} J_{0,1}(\omega_{\alpha}) \delta \omega, \quad (8)$$

where $\delta \omega$ is the increment used to discretize the spectral density. In all calculations shown below we choose the cut-off parameter $\gamma = 5$ in atomic units. In performing the calculations, we have checked for the convergence with respect to the number of modes by increasing N_b until no further change in the Fourier transforms of the calculated correlation functions (i.e., absorption spectra) was observed. The results reported below were obtained by setting $N_b = 100$.

III. VIBRONIC ABSORPTION SPECTRUM

We calculate the electronic spectrum within the Fermi golden rule and the electric dipole approximation.²¹ The normalized electronic absorption spectrum is given by the Fourier transform of the real-time dipole autocorrelation function

$$I(\omega) = \frac{1}{2\pi} \int_{-\infty}^{\infty} dt \exp(i\omega t) C(t), \quad (9)$$

where the real-time dipole autocorrelation function is given by

$$C(t) = \frac{\text{Tr}[e^{-\beta H} e^{iHt/\hbar} \mu e^{-iHt/\hbar} \mu]}{\text{Tr}[e^{-\beta H} \mu^2]}, \quad (10)$$

$\beta = 1/k_B T$, $\text{Tr}(\cdots)$ denotes the trace over all nuclear and electronic degrees of freedom, and μ is the transition-dipole operator.

Within the Condon approximation, μ does not depend on the nuclear coordinates. Hence we replace the transition-dipole operator with

$$\mu = \mu_{01}|0\rangle\langle 1| + \mu_{10}|1\rangle\langle 0|. \quad (11)$$

We will limit the discussion to temperatures much lower than the electronic energy gap ($\hbar \omega_e \gg kT$). Carrying out the trace over the electronic states results in

$$C(t) = \langle e^{iH_0 t/\hbar} e^{-iH_1 t/\hbar} \rangle. \quad (12)$$

In the above, $\langle \cdots \rangle = \text{Tr}_{\mathbf{x}}(\rho_0 \cdots)$ denotes the trace only over the nuclear coordinates and $\mathbf{x} \equiv (q, \mathbf{Q})$. The equilibrium density operator is approximated by

$$\rho_0 = \frac{1}{Z(\beta)} e^{-\beta(h_0(q) + H_b(\mathbf{Q}))}, \quad (13)$$

where $Z(\beta)$ is the partition function

$$\begin{aligned} Z(\beta) &= \text{Tr}_{\mathbf{x}}[e^{-\beta(h_0(q) + H_b(\mathbf{Q}))}] \\ &= \int d\mathbf{x} \langle \mathbf{x} | e^{-\beta(h_0(q) + H_b(\mathbf{Q}))} | \mathbf{x} \rangle. \end{aligned} \quad (14)$$

We have made an assumption that the initial density can be written as a product of the system density and the bath density, i.e., we factorize the initial conditions.^{22–25} We find that this approximation for the initial density does not influence the long-time behavior (which is reflected in the structure of the individual features of the vibronic absorption spectrum) of the dipole autocorrelation function for the set of parameters studied here. We will further elaborate on this point in a future publication.²⁶

Within the Fermi golden rule given above, the real-time dipole autocorrelation functions for our model can be calcu-

lated exactly.¹⁷ We are interested in the solution for $C(t)$ for the following three cases, which were extensively discussed in our previous work (readers interested in the details of the calculations should consult Ref. 17):

- (1) The fully quantum mechanical (FQM) results are obtained by employing the density matrix formalism of Kubo and Toyozawa,²⁷ or alternatively the boson algebra technique of Balian and Brezin.²⁸
- (2) A semiclassical approximation in which the dynamics of all nuclear degrees of freedom (system and bath) are treated classically, while the two electronic states are treated quantum mechanically. We use two alternative propagation schemes for the classical degrees of freedom; one on the ground electronic state [the dynamical classical limit (DCL)], and the other on the arithmetic averaged Hamiltonian [the averaged classical limit (ACL)].^{9,17} The results for both approximations are obtained by a method developed in our previous work,¹⁷ which is based on Gaussian integrals and normal mode propagation.
- (3) A mixed quantum-classical (MQC) approximation in which the system vibrational mode (in addition to its electronic states) is treated quantum mechanically, while the bath is treated in the dynamical classical limit. The effect of the bath on the spectrum in this approach is entirely given by the influence functional of Feynman and Vernon,²⁹ which was generalized for the present problem by Egorov, Rabani, and Berne.¹⁷

In the next section we will present results obtained for the dipole autocorrelation function and the vibronic absorption spectrum for all three cases mentioned above.

IV. RESULTS AND DISCUSSION

We are primarily interested in the regime where the electronic dephasing rate is slower than the vibrational relaxation rate ($T_1^{\text{vib}} < T_2^{\text{elec}}$). In Fig. 1 we compare the two rates as a function of the coupling strength on the ground electronic state ρ_0 . When the frequencies in the two electronic states are the same (lower panel), the electronic dephasing rate depends on the magnitude of the difference between the coupling strength $\rho_1 - \rho_0$ [see Eq. (72) of Ref. 17], while the vibrational relaxation rate in each of the electronic states depends on the magnitude of the coupling strength ($1/T_1^{\text{vib}} = \pi J_{0,1}(\omega_{0,1})/\omega_{0,1}$). The situation is somewhat more complex when the frequencies in the two electronic states are different (upper panel). It is clearly seen in the figure that the condition $T_1^{\text{vib}} < T_2^{\text{elec}}$ can be satisfied for various sets of system–bath parameters. For the calculations reported below we use (from now on we employ atomic units) $\rho_0 = 0.25$ and $\rho_1 = 0.24$ for $\omega_0 = \omega_1 = 1.0$, and $\rho_0 = 0.38$ and $\rho_1 = 0.24$ for $\omega_0 = 1.16$ and $\omega_1 = 0.92$. Both sets of parameters are chosen to ensure that $T_1^{\text{vib}} < T_2^{\text{elec}}$.

A. Vibronic absorption spectra

We now turn to the discussion of the vibronic absorption spectrum given by the Fourier transform of the dipole autocorrelation function [cf. Eq. (9)]. We have calculated $I(\omega)$ for two values of $\delta = q_1 - q_0$ (the relative shift in the equi-

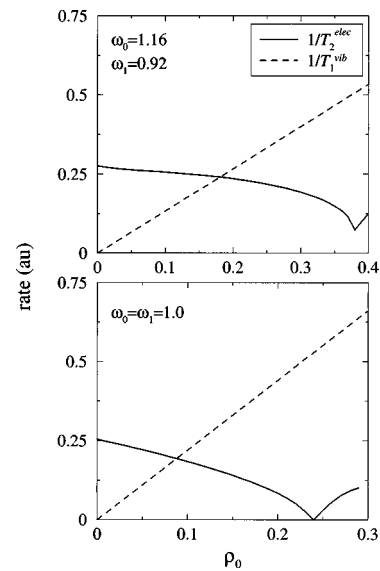


FIG. 1. A plot of the electronic dephasing rate, $1/T_2^{\text{elec}}$, and the vibrational relaxation rate on the ground electronic state, $1/T_1^{\text{vib}}$, versus the coupling strength in the ground electronic state, ρ_0 . The lower panel is for $\omega_0 = \omega_1 = 1.0$, and the upper panel is for $\omega_0 = 1.16$ and $\omega_1 = 0.92$. Both panels are for an inverse temperature of $\beta = 1.0$, and the coupling on the excited electronic state is $\rho_1 = 0.24$. Note that $1/T_2^{\text{elec}}$ decreases with ρ_0 until a minimum is reached, and then it increases with ρ_0 , while $1/T_1^{\text{vib}}$ scales linearly with the coupling strength.

librium position of the system vibrational mode in the two electronic states). The results are shown in Figs. 2 and 3 for vibrational frequencies of $\omega_0 = \omega_1 = 1.0$ and $\omega_0 = 1.16$, $\omega_1 = 0.92$, respectively.

When the vibrational frequencies are the same for the two electronic states, the averaged classical limit (ACL) is indistinguishable from the fully quantum mechanical (FQM) result, and therefore is not shown in Fig. 2. In the absence of “shifts” in the equilibrium positions, the vibronic absorption

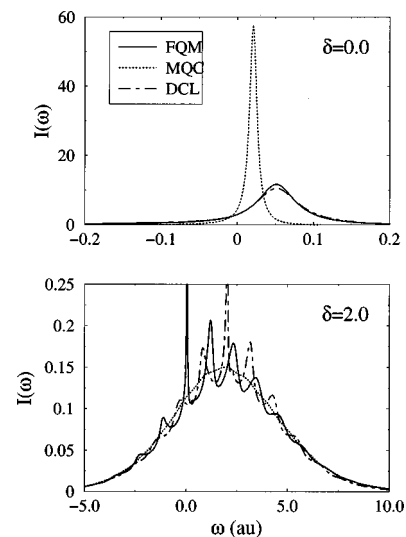


FIG. 2. Plots of the vibronic absorption spectrum of a diatomic molecule coupled to a harmonic bath for two different relative shifts in the equilibrium position of the primary mode. The coupling strengths are $\rho_0 = 0.25$ and $\rho_1 = 0.24$, and the vibrational frequencies ω_0 and ω_1 are set equal to unity. Note the poor agreement between the MQC and FQM results.

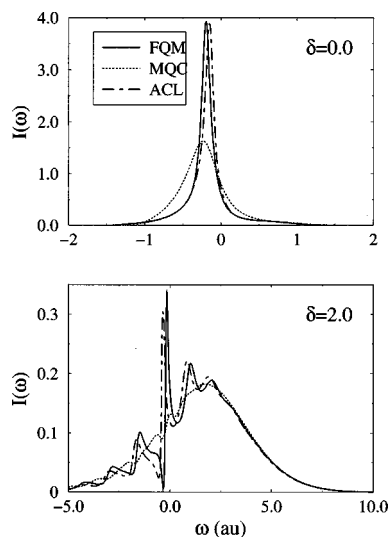


FIG. 3. Plots of the vibronic absorption spectrum of a diatomic molecule coupled to a harmonic bath for two different shifts in the equilibrium position of the primary mode. The coupling strengths are $\rho_0=0.38$ and $\rho_1=0.24$, and the vibrational frequencies are taken to be different in the two electronic states ($\omega_0=1.16$ and $\omega_1=0.92$).

spectrum is structureless. It is clearly seen that the mixed quantum-classical (MQC) approximation in the limit of fast vibrational relaxation breaks down. The MQC underestimates the width and the shift of the absorption spectrum. This is in contrast to our previous observation for slow vibrational relaxation,¹⁷ in which case the MQC approximation was superior in overall performance as compared to other semiclassical approximations. The breakdown is even more pronounced when “shifts” in the equilibrium positions of the system are included. The MQC approximation only captures the envelope of the spectrum, and fails to predict the individual vibronic features. We find that for the low temperature studied here, the MQC starts to break down when the electronic dephasing rate is slightly below the vibrational relaxation rate. As expected based on the work of Bader and Berne,¹⁸ the problems with MQC are somewhat less pronounced for higher temperatures.

The dynamic classical limit (DCL) is in good agreement with the FQM results in the absence of “shifts” in the equilibrium positions. When the “shifts” are included, the DCL does capture the overall shape and width of the individual vibronic features; however, they are shifted with respect to the FQM results.¹⁷

It is interesting to examine a more general case when the system vibrational frequencies in the two electronic states are different. In Fig. 3 we plot the absorption spectrum for such a case. The DCL results are essentially the same as for the previous case (i.e., the widths of the individual features are slightly overestimated and their positions are shifted), and hence are not shown for the clarity of presentation.

Once again the MQC approximation in the absence of “shifts” in the equilibrium positions fails to agree with the FQM results; however, for this set of parameters it overestimates the width of the absorption spectrum. When the “shifts” in the equilibrium positions are included, the MQC approximation does exhibit a vibronic structure, unlike the

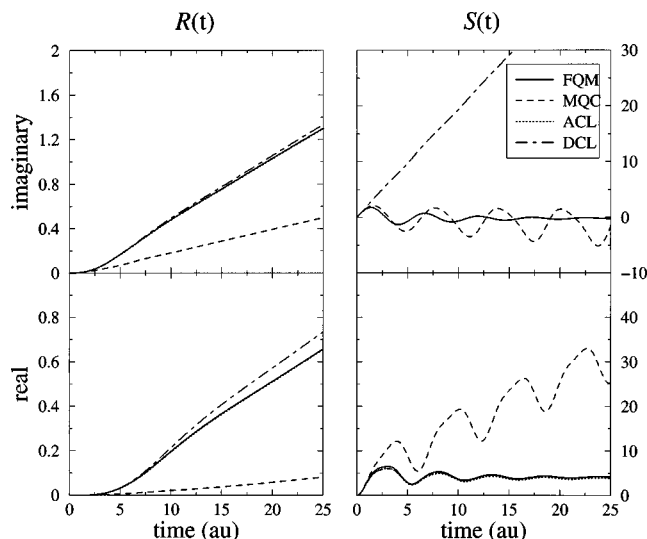


FIG. 4. Plots of the real and imaginary part of the “rotation” (left panels) and “shift” (right panels) functions for the FQM results and all the semiclassical approximations. The vibrational frequencies ω_0 and ω_1 are set equal to unity, the relative shift in the equilibrium position is $\delta=2.0$, and the coupling strengths are $\rho_0=0.25$ and $\rho_1=0.24$. The ACL is indistinguishable from the FQM results, while the MQC approximation provides the worst agreement with the FQM results.

case when $\omega_0=\omega_1$; however, it clearly overestimates the width of individual features, and also some are misplaced.

The averaged classical limit (ACL) is not exact for this choice of parameters, as can be clearly seen in Fig. 3. Nevertheless, this approximation provides good agreement with the FQM results, although the individual lines are somewhat misplaced.

B. Dipole autocorrelation function

In this subsection we consider the origin of the discrepancies between various semiclassical approximations and the fully quantum mechanical results. To this end, we perform a detailed examination of the time-dependent dipole autocorrelation function. In our previous work¹⁷ we have introduced the “rotation” $[R(t)]$ and “shift” $[S(t)]$ functions, which are associated with the rotation between the normal modes of each electronic state and the shifts in their equilibrium positions, respectively. In terms of these functions, the dipole autocorrelation function takes a very simple form: $\ln[C(t)] = R(t) + S(t)$. When the coupling between the system and the bath in the two electronic states is the same, the “rotation” term vanishes $[R(t)=0]$, and when the shifts in the equilibrium positions in the two electronic states are the same, the “shift” term vanishes $[S(t)=0]$. Hence, these functions simplify the interpretation of the results in the time domain.

In Figs. 4 and 5 we plot $R(t)$ and $S(t)$ for the set of parameters used in Figs. 2 and 3, respectively. The results shown are for $\beta=1.0$ and $\delta=2.0$. The “rotation” term does not depend on the value of δ and the “shift” term vanishes when $\delta=0.0$; therefore, we do not display the results for the latter case. All three semiclassical approximations provide good agreement with the FQM results at short times. This reflects the good agreement for the envelope of the vibronic absorption spectrum shown in the previous plots.

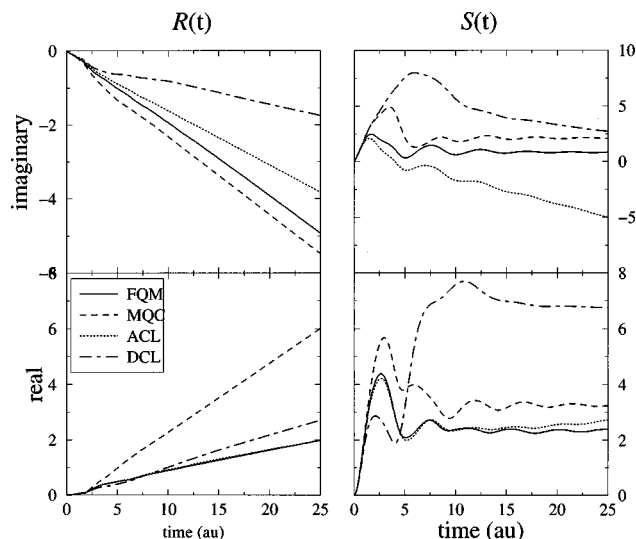


FIG. 5. The same as Fig. (4) but for the case of different system frequencies for the two electronic states, $\omega_0=1.16$ and $\omega_1=0.92$. The coupling strengths are $\rho_0=0.38$ and $\rho_1=0.24$.

As mentioned earlier, when $\omega_0 = \omega_1$, the ACL is essentially exact. The small discrepancy between the ACL and FQM results can be traced to the difference in the thermal probability used to perform the averaging. The agreement between the ACL and the FQM results is very good for the “rotation” term, even when the frequencies are different in the two electronic states; however, the imaginary part of the “shift” term has an additional time-dependent linear term, which is responsible for the small shift of the ACL spectrum (Fig. 3).

The intermediate and long-time behavior of the dynamical classical “rotation” term (DCL) is qualitatively similar to the FQM “rotation” term. The slopes of the real part of $R(t)$ are slightly different for both sets of parameters; however, the imaginary part of $R(t)$ deviates significantly from the FQM results when the two system frequencies are different. Regarding the DCL “shift” term, we observe that at long times the real part follows the FQM results when $\omega_0 = \omega_1$, but deviates significantly when $\omega_0 \neq \omega_1$. The imaginary part of the “shift” term displays a linear time dependence at long times (which is not seen when the frequencies are different since this effect steps in at later times); however, unlike the averaged classical “shift” term, which exhibits this linear dependence only when $\omega_0 \neq \omega_1$, the linear term exists for both sets of frequencies in the DCL. This fact explains a relatively large shift in the DCL vibronic absorption spectra shown in Figs. 2 and 3.

The MQC approximation provides the worst agreement with the FQM results, in contrast to the case when the electronic dephasing rate is faster than the vibrational relaxation rate. This is clearly seen in the real parts of the “rotation” terms which are markedly below their FQM counterparts when $\omega_0 = \omega_1$, and above these when $\omega_0 \neq \omega_1$. This mismatch is the cause for the large discrepancy in the width of the absorption line in the absence of shifts in the equilibrium positions. In addition to that, we find that the real and imaginary parts of the “shift” function oscillate in a much more

pronounced way as compared to the FQM case, and the amplitude of the oscillations increases with time. The situation is somewhat better when $\omega_0 \neq \omega_1$, mainly due to the smaller ratio between the electronic dephasing rate and the vibrational relaxation rate.

V. CONCLUSIONS

In this paper we have extended our study of the vibronic absorption spectrum of a diatomic molecule coupled to a bath,¹⁷ in order to assess the accuracy of several semiclassical approximations. We have focused on the limit of fast vibrational relaxation compared to the electronic dephasing, in order to establish a connection with the results obtained for semiclassical treatments of vibrational energy relaxation processes.^{18–20}

In our previous work we have shown that the mixed quantum-classical treatment for the vibronic absorption spectrum provides the best overall agreement with the fully quantum mechanical results for a large range of system–bath parameters. This seems surprising in view of the conclusions reached by Bader and Berne,¹⁸ and by others,^{19,20} according to which the fully classical treatment is superior to the mixed one in the context of vibrational energy relaxation. However, the results of Ref. 17 were obtained for the range of parameters where the decay of the real-time dipole autocorrelation function was completely dominated by the electronic dephasing, and not by the vibrational energy relaxation (i.e., $1/T_2^{\text{elec}} > 1/T_1^{\text{vib}}$).

In the present work we have shown that the mixed quantum-classical treatment breaks down when the vibrational relaxation rate is larger than the electronic dephasing rate ($1/T_2^{\text{elec}} < 1/T_1^{\text{vib}}$), which is consistent with the predictions made for vibrational relaxation processes.^{18–20} We find that the condition ($1/T_2^{\text{elec}} < 1/T_1^{\text{vib}}$) can be satisfied for a wide range of system–bath parameters. For more realistic system models, we anticipate that the above condition can occur when, for example, the change in the molecular dipole upon excitation is small, but the molecule is strongly coupled to the bath in both electronic states. However, this is not the only case for which the mixed quantum-classical approximation breaks down, since the condition ($1/T_2^{\text{elec}} < 1/T_1^{\text{vib}}$) can occur for a wide range of system and bath parameters. Therefore, for realistic systems, one must estimate T_2^{elec} and T_1^{vib} prior to applying a detailed mixed quantum-classical treatment.

We also find that the average classical limit provides the best overall agreement with the fully quantum mechanical results (when $1/T_2^{\text{elec}} < 1/T_1^{\text{vib}}$), although the individual vibronic features in the spectrum are slightly misplaced. The good agreement between the averaged classical limit and the fully quantum mechanical results is expected based on the phase-space analysis of the Wigner transform as given in Ref. 17. A detailed examination of the phase-space equations reveals the fact that the averaged classical limit might also break down for more realistic systems, which are not described by the quadratic model.

Bader and Berne¹⁸ have shown that the vibrational relaxation rate on a given electronic state harmonic surface is

identical for the fully quantum mechanical and fully classical treatments of the nuclear motion, and is very poorly approximated by a mixed ensemble in which the molecular nuclear motion is treated quantum mechanically and the bath nuclear motions are treated classically. Their observation provides an explanation for the breakdown of the mixed quantum-classical approximation and for the success of the averaged classical limit here, since the vibronic absorption spectrum is dominated by the vibrational relaxation processes in the above regime ($1/T_2^{\text{elec}} < 1/T_1^{\text{vib}}$).

Finally, we would like to point out that our conclusions are based on a quadratic model for the nuclear degrees of freedom. Nevertheless, the failure of the semiclassical treatments for our simple model indicates potential problems in the use of such treatments for more complex systems.

ACKNOWLEDGMENTS

E.R. acknowledges the Rothschild and Fulbright foundations for financial support. This work was supported by a grant to B.J.B. from the National Science Foundation.

¹*Spectroscopy and Excitation Dynamics of Condensed Molecular Systems*, edited by V. M. Agranovich and R. M. Hochstrasser (North-Holland, Amsterdam, 1983).

²S. Mukamel, *Principles of Nonlinear Optical Spectroscopy* (Oxford University Press, Oxford, 1995).

- ³J. L. Skinner and W. E. Moerner, *J. Phys. Chem.* **100**, 13,251 (1996).
⁴S. Mukamel, *J. Chem. Phys.* **77**, 173 (1982).
⁵D. Chandler, K. S. Schweizer, and P. G. Wolynes, *Phys. Rev. Lett.* **49**, 1100 (1982).
⁶D. Thirumalai, E. J. Bruskin, and B. J. Berne, *J. Chem. Phys.* **83**, 230 (1985).
⁷D. G. Evans and R. D. Coalson, *J. Chem. Phys.* **97**, 5081 (1992).
⁸L. E. Fried and S. Mukamel, *J. Chem. Phys.* **96**, 116 (1992).
⁹N. E. Shemetulskis and R. F. Loring, *J. Chem. Phys.* **97**, 1217 (1992).
¹⁰K. Haug and H. Metiu, *J. Chem. Phys.* **99**, 6253 (1993).
¹¹J. G. Saven and J. L. Skinner, *J. Chem. Phys.* **99**, 4391 (1993).
¹²R. M. Stratt and J. E. Adams, *J. Chem. Phys.* **99**, 775 (1993).
¹³J. E. Adams and R. M. Stratt, *J. Chem. Phys.* **99**, 789 (1993).
¹⁴A. Heidenreich and J. Jortner, *J. Chem. Phys.* **105**, 8523 (1996).
¹⁵S. A. Egorov, E. Gallicchio, and B. J. Berne, *J. Chem. Phys.* **107**, 9312 (1997).
¹⁶I. Benjamin, *Chem. Phys. Lett.* **287**, 480 (1998).
¹⁷S. A. Egorov, E. Rabani, and B. J. Berne, *J. Chem. Phys.* **108**, 1407 (1998).
¹⁸J. S. Bader and B. J. Berne, *J. Chem. Phys.* **100**, 8359 (1994).
¹⁹S. A. Egorov and B. J. Berne, *J. Chem. Phys.* **107**, 6050 (1997).
²⁰J. L. Skinner, *J. Chem. Phys.* **107**, 8717 (1997).
²¹R. G. Gordon, *Adv. Magn. Reson.* **3**, 1 (1968).
²²J. L. Skinner and D. Hsu, *J. Phys. Chem.* **90**, 4931 (1986).
²³D. Hsu and J. L. Skinner, *J. Lumin.* **37**, 331 (1987).
²⁴D. R. Reichman and R. J. Silbey, *J. Chem. Phys.* **104**, 1506 (1996).
²⁵N. Makri and D. E. Makarov, *J. Chem. Phys.* **102**, 4600 (1995).
²⁶S. A. Egorov, E. Rabani, and B. J. Berne (unpublished).
²⁷R. Kubo and Y. Toyozawa, *Prog. Theor. Phys.* **13**, 160 (1955).
²⁸R. Balian and E. Brezin, *Nuovo Cimento* **64**, 37 (1969).
²⁹R. P. Feynman and F. L. Vernon, *Ann. Phys. (N.Y.)* **24**, 118 (1963).